Ophthal. Physiol. Opt. 2004 **24:** 419–426

Comparison of aberrations in different types of progressive power lenses

Eloy A. Villegas and Pablo Artal

Laboratorio de Optica, Departamento de Física, Universidad de Murcia, Campus de Espinardo (Edificio C), Murcia, Spain

Abstract

Recently, computer numerically controlled machines have permitted the manufacture of progressive power lenses (PPLs) with different designs. However, the possible differences in optical performance among lens designs are not yet well established. In this work, the spatially resolved aberrations, at 20 relevant locations, of three PPLs with different designs were measured with a Hartmann–Shack wavefront sensor. The wavefront aberration (WA), its root mean square error (RMS) and the point-spread function were obtained. Spatially resolved plots are shown for all aberrations, astigmatism alone, and for higher order aberrations. The average RMS of all zones is also compared, and the standard deviation is used as a parameter to evaluate the level of hard-soft design. We find differences in the spatial distribution of the aberrations but not in the global RMS, indicating that current PPLs are rather similar to a waterbed, with the aberrations being the water: they can be moved but they cannot be eliminated.

Keywords: current designs, Hartmann-Shack sensor, optical performance, progressive addition lenses, progressive power lenses, wavefront aberration

Introduction

Progressive addition lenses (PALs) or, as we will refer to them within this paper, progressive power lenses (PPLs) are a common and successful optical solution for presbyopia. Many different types of PPLs have been designed and manufactured since this technology became available in the 1950s. A problem of PPLs is the presence of peripheral astigmatism induced by the continuous change in power through the lens. Astigmatism degrades vision through some parts of the lens and may play a role in reducing the success of the adaptation process. This issue was well recognized from the early days: Minkwitz (1963) stated that it was not possible to produce a progressive spherical power surface without astigmatism and distortion being present at some point. Despite numerical control lathe machines being able to generate aspheric surface sections, which minimize peripheral astigmatism, current PPL designs still present significant amounts of this aberration. Beyond astigmatism, the impact of other higher order aberrations in PPLs has been much less studied. In a recent study (Villegas and Artal, 2003), we measured wave-aberrations at different locations of a PPL and the coupling with the aberrations of the eye. In addition to astigmatism, small amounts of other aberrations, mainly coma and trefoil, were also present in the lens.

The PPL designs are commonly described according to the astigmatism distribution over the progressive surface. PPLs are grouped into either hard or soft progressive designs (Jalie, 2001). The lenses with hard design have wide astigmatism-free far and near vision areas, but astigmatism rapidly increases away from the corridor in the intermediate zones. In the soft design, the astigmatism-free far and near areas are narrower but are introduced at a more gradual pace, with a slower increase of astigmatism in lateral zones. First generation PPLs had a symmetrical distribution of astigmatism around the corridor (symmetric design). However, since in normal binocular vision the eyes move a slightly

Received: 30 September 2003
Revised form: 29 March 2004
Accepted: 19 April 2004

Correspondence and reprint requests to: Eloy A. Villegas.
E-mail address: villegas@um.es

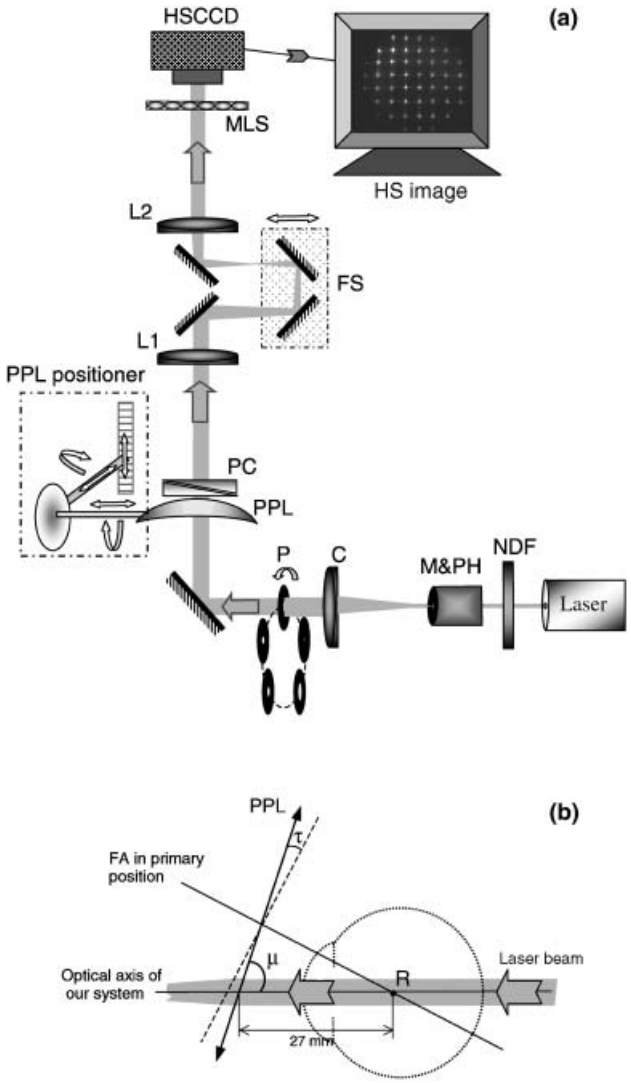

Figure 1. (a) Experimental setup. NDF, variable neutral density filters; M&PH, microscope objective and pinhole; C, collimator achromatic lens; P, revolver of apertures; PPL, progressive power lens; PC, prism compensator; L1 and L2, achromatic lenses; FS, focus corrector system; MLS, microlenses; HSCCD, CCD to capture Hartmann–Shack images. (b) Simulation in our system of the PPL tilt for a near vision zone. The dotted contour represents the position of the eye with respect to the lens in normal viewing. FA, fixation axis; τ, pantoscopic tilt; μ, angle between lens and FA; R, centre of rotation of the eye.

larger distance on the temporal side of a lens than on the nasal side, an asymmetric design was proposed in which astigmatism changed more gradually towards the temporal area of the lenses (Tunnacliffe, 1995). Moreover, for most PPL designs, the distribution of unwanted astigmatism varies with the addition power.

Subjective assessment of PPLs is commonly undertaken in two ways, by psychophysical measurements (Sullivan and Fowler, 1989) or by surveys to evaluate patient acceptance and satisfaction (Cho *et al.*, 1991: Gresset, 1991). These experiments require the

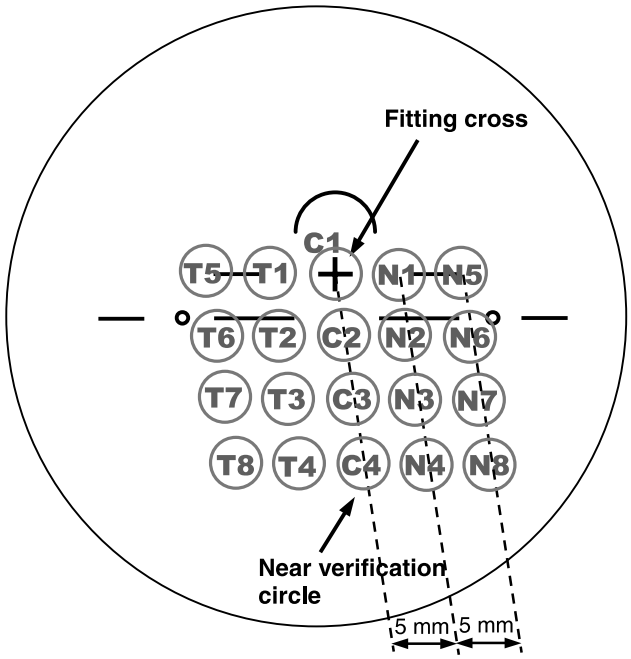

Figure 2. Measured zones in the PPLs with 4.0-mm in diameter.

collaboration of the subjects. In particular, obtaining accurate psychophysical results is time-consuming. Although the surveys are often quite useful for comparing different PPLs, the lack of control over the process may lead to biased results. However, different PPLs can be measured using lensmeters (Sheedy *et al.*, 1987; Diepes and Tameling, 1988) to obtain the distribution of the power and astigmatism. In these studies, significant differences between various types of PPLs were found. A recent work (Han *et al.*, 2003) suggests that eye and head movements may at times discriminate between different designs of PPLs.

Although many authors have proposed different optical methods for designing and evaluating PPLs (Fowler and Sullivan, 1989; Bourdoncle *et al.*, 1992; Rosenblum *et al.*, 1992; Atchison and Kris, 1993; Castellini *et al.*, 1994; Liu, 1994; Burns, 1995; Alonso *et al.*, 1997; Loos *et al.*, 1998; Spiers and Hull, 2000; Quiroga *et al.*, 2001), there is a significant lack of studies presenting objective measurements on different PPL designs. In this context, we have measured spatially resolved wavefront aberrations (WA) in central and peripheral locations (up to $\pm 20°$ from far to near areas) of three different types of PPL currently available. Aberrations and optical quality parameters are compared and a brief discussion on the design philosophy of the different lenses is also included.

Methods

There are different methods for measuring and evaluating the optical quality of ophthalmic lenses. Optical

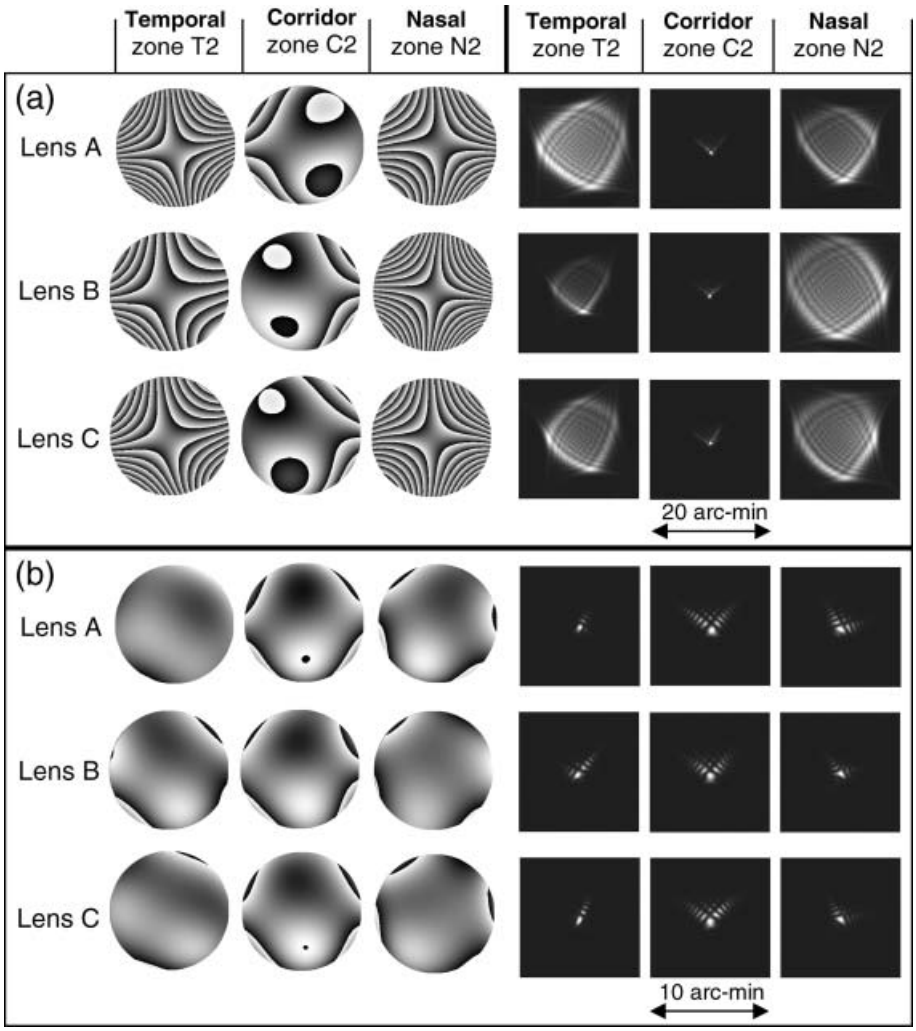

Figure 3. A modulus 2π representation of the WA maps and the associated PSFs, at three intermediate zones (C_2 at the corridor, N_2 and T_2 at the nasal and temporal side), as examples of the twenty tested zones, for each PPL. (a) Considering defocus zero. (b) Considering defocus and astigmatism zero. 6.0-mm pupil diameter.

bench measurements include interferometry (Malacara, 1992), Ronchi test (Gonzalez *et al*., 1997) or Moiré deflectometry (Rottenkolber and Podbielska, 1996). These techniques were used to estimate the optical quality of the isolated lenses. We used a Hartmann–Shack (HS) wavefront sensor, specially designed and built to measure spatially resolved aberrations. This technique allows for measurement of high-order aberrations while conventional lensmeters can only measure defocus and astigmatism. Our system has been designed to measure the aberrations of the ophthalmic lens either in isolation or in combination with the eye (Villegas and Artal, 2003). We measured three different types of PPL at different locations within the lens that was positioned and tilted in the system to resemble natural viewing conditions.

Figure 1a shows a schematic diagram of the HS wavefront sensor in the configuration to measure isolated PPLs. The principle of operation of the HS sensor has been extensively described elsewhere (Liang *et al*., 1994; Prieto *et al*., 2000). In brief, our particular implementation (Villegas and Artal, 2003) is as follows. A green (543 nm) He-Ne laser beam first passes through a neutral density filter (NDF) that controls the light intensity. A spatial filter, with a 20× microscope objective and a 10-μm pinhole, produces a point-like source. Lens C collimates the beam that passes through a size-adjustable aperture (P). The beam is directed to the posterior surface of the tested PPL. The aberrations of the PPL can be coupled to those of the eye measured with a HS sensor (Villegas and Artal, 2003). A three-stage micro-positioner allows both tilt and movement of the lens to reproduce the actual position of the lens in front of eye and to select the different parts of the lens.

To estimate the displacements and the tilts, the distance between the back vertex of the PPL and the centre of rotation of the eye was assumed as 27 mm and the pantoscopic tilt as 12°. *Figure 1b* represents

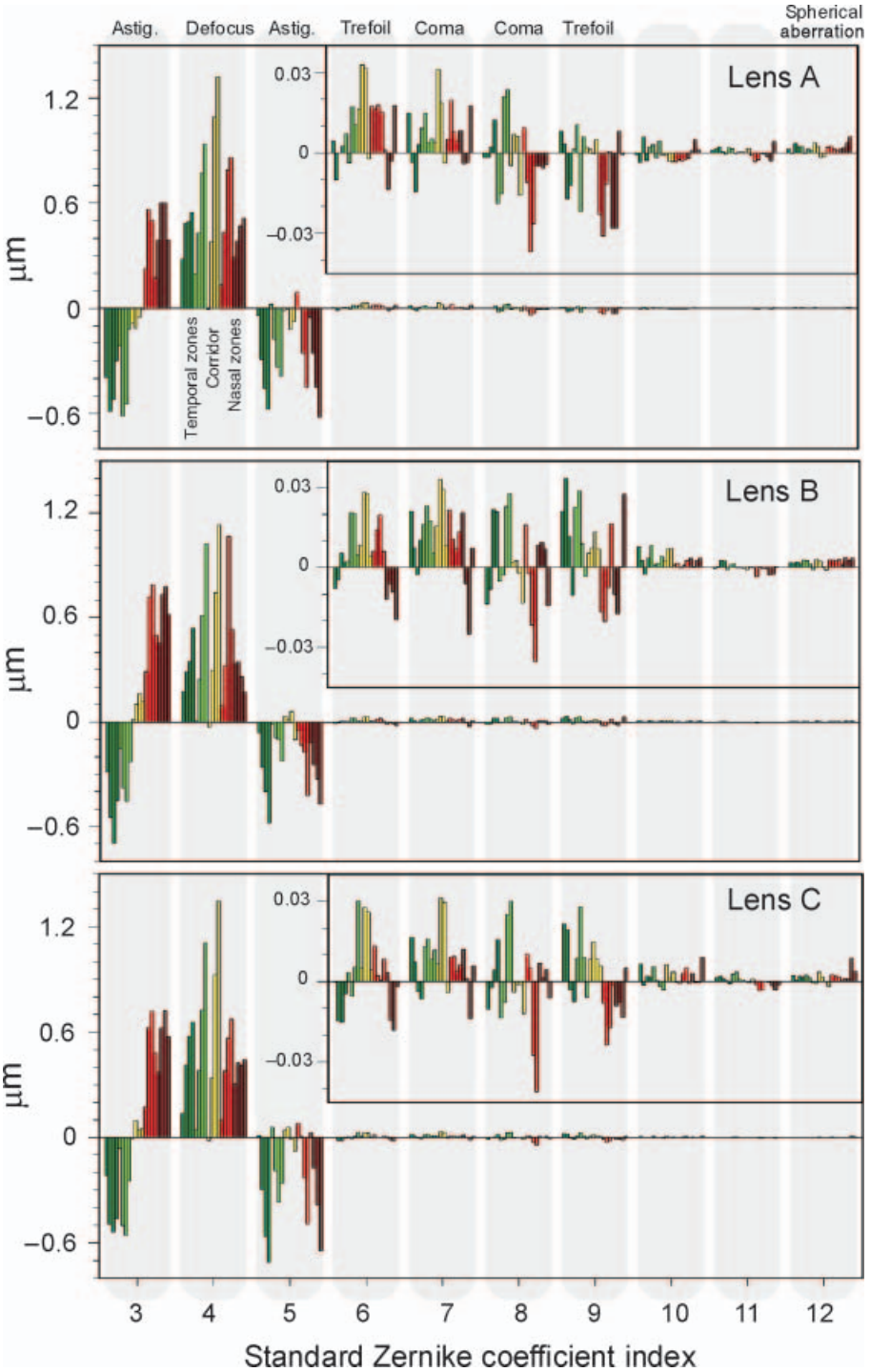

Figure 4. Zernike coefficients for the tested locations (for 4-mm diameter zones) of the three progressive lenses: in the corridor (yellow bars), 5 mm away from corridor (red bars for nasal zones and green bars for temporal zones) and 10 mm from corridor (dark red bars for nasal zones and dark green bars for temporal zones). Bars from left to right correspond to zones from far to near. The high order coefficients (from coefficient 6 to 12) are also shown on a larger scale. The Seidel aberrations corresponding to Zernike coefficients are noted on top of the figure.

schematically how the PPLs were placed in the system for a near zone. The tested zone of the PPL is located at one focal distance of the lens L1 to be conjugated with the microlens array (MLS). If a large prismatic effect is induced by the PPL, the prism compensator (PC) realigns the beam. A focus corrector sub-system (lenses L1 and L2, and two mirrors on a moving stage) compensates for defocus allowing reliable aber-

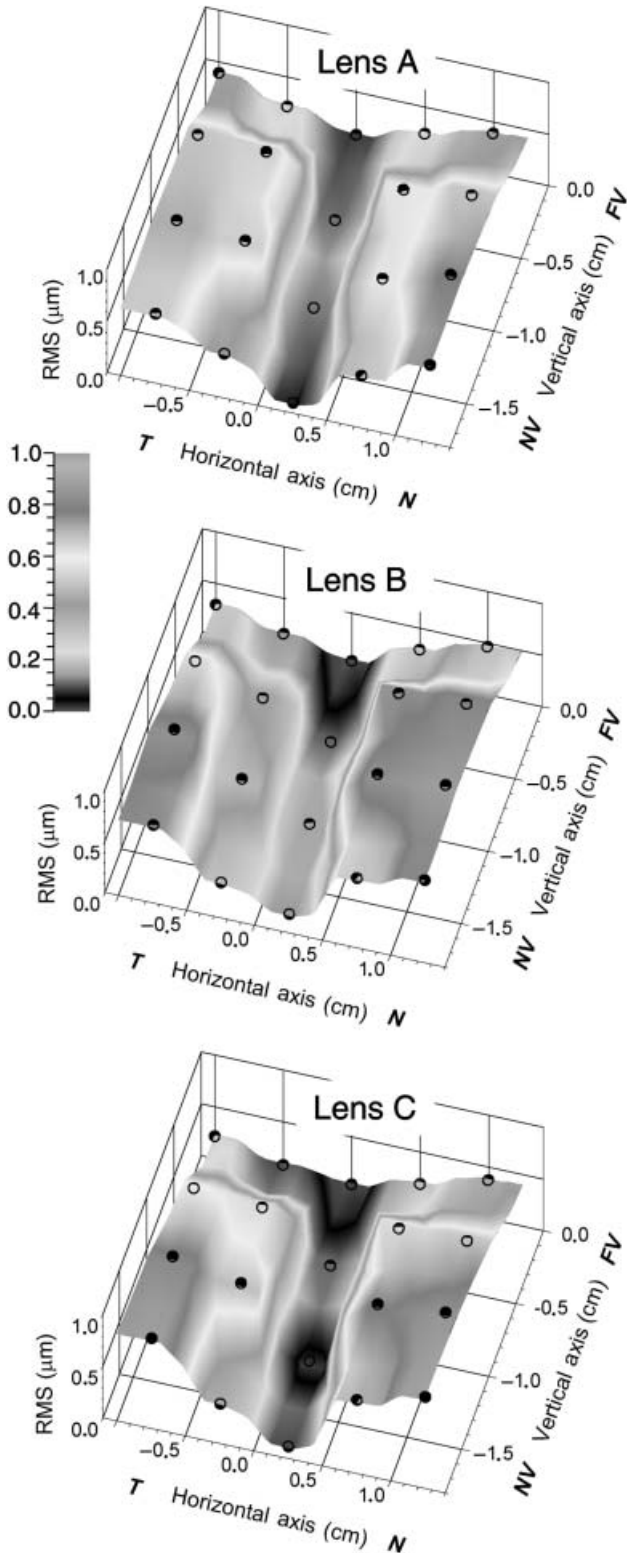

Figure 5. Spatially resolved RMS for 4.0-mm pupil diameter, considering defocus zero.

ration measurements under every condition. The beam coming from L2 is sampled by the MLS (square geometry, 40-mm focal length, single microlens aperture of 0.6 mm). HS images are recorded by a cooled CCD camera (HSCCD) placed at the focus position of the MLS.

From the HS images, WA are fitted to Zernike polynomials using a procedure described elsewhere (Prieto *et al*., 2000). WAs were reconstructed for a 6-mm pupil size at the PPL plane. For this pupil, 30–36 spots in the HS image are analysed allowing a Zernike decomposition up to fifth order. From the 6-mm pupil WA, the aberrations were also computed for a smaller 4-mm pupil diameter by selecting the appropriate area. Zernike coefficients and the root mean square (RMS) of the WA for every tested zone were obtained. The point-spread functions (PSF) are also calculated from the WA. We used a 4 mm pupil size because larger pupils are uncommon in presbyopic eyes. However, to see the effect of aberrations more clearly, WA and PSF maps are shown for the 6-mm pupil diameter.

We measured three different PPLs that are commercially available and marketed as recent designs. The main goal of this study is to evaluate the optical quality of current PPL designs and to show the differences between them. As we do not have any commercial interest in any product, the lenses tested in this study are simply called A, B and C. The three lenses have in common the following characteristics: the progressive surface is on the front of the lens; glass material of refractive index 1.6; plano distance power; 2D power addition; 18-mm corridor length (vertical measurement from the fitting cross to the centre of the near verification circle); and 2.5-mm inset of the near portion. For each of the three PPLs, the WA was measured in 20 zones spatially distributed as a 5×4 array of locations: a column along the corridor and at both sides (nasal and temporal) two columns 5 and 10 mm away from corridor. *Figure 2* shows the locations of these measurement zones on the lens surface. Zones along the corridor are noted as C_i and those at the temporal and nasal side as T_i and N_i respectively. In order to better show the spatially resolved optical properties of the lenses, mesh and contour plots for a rectangular area of the lenses are generated from interpolation of values of the 20 tested zones using an inverse distance method.

Results

As an example of the type of results obtained, *Figure 3a* shows the WA and PSF maps (with defocus set to zero) for three zones in intermediate vision (C_2 at the corridor, N_2 and T_2 at the nasal and temporal side 5-mm away from corridor) of the three tested PPLs for a 6-mm pupil diameter. The PSFs are calculated at the circle of least confusion. For every lens, typical comatic shapes appear in the corridor zone. In the zones outside the corridor, astigmatism increases and becomes the

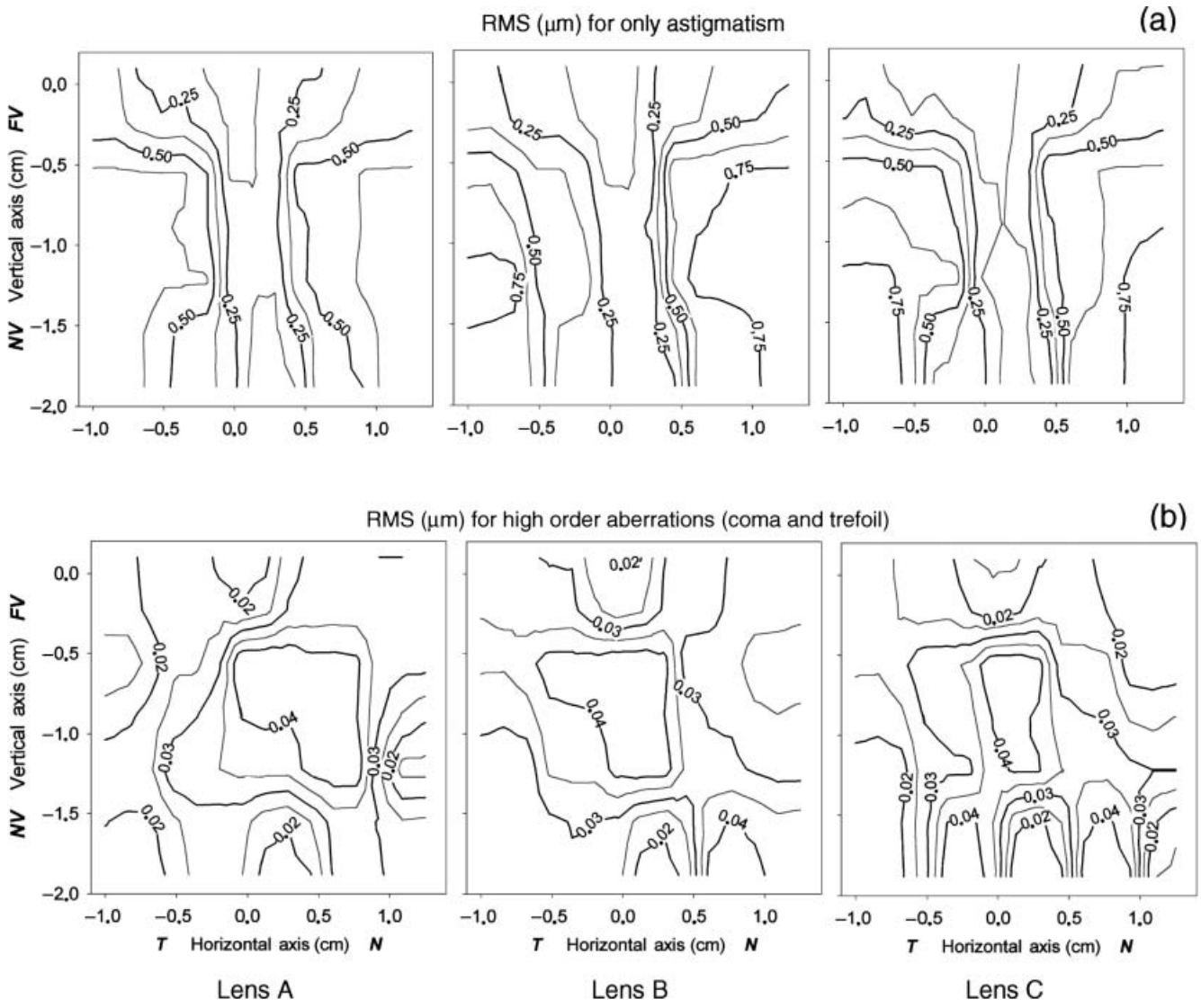

Figure 6. (a) Contour plots of RMS considering only astigmatism, with 4.0-mm pupil size. (b) RMS for higher order aberrations, mainly coma and trefoil, because the other higher order aberrations are negligible.

dominant aberration, although the amount of astigmatism is different for each lens. *Figure 3b* shows the same results but without astigmatism; i.e. both defocus and astigmatism set to zero. This represents the impact of higher order aberrations. In addition to coma, a small amount of trefoil is also present in every case. It is interesting to note that the orientation of coma changes from vertical in the corridor to an oblique direction in the peripheral zones, due to the defocus decrease outside the corridor.

The values of the Zernike coefficients for all tested zones of the three PPLs are presented in *Figure 4*. The evolution of defocus over the lenses is shown by coefficient 4. This coefficient and those corresponding to astigmatism (coefficients 3 and 5) are slightly different between the lenses. The magnitude and type of high order aberrations is similar for the three different lenses evaluated. The most important high order aberrations are coma (coefficients 7 and 8) and trefoil (coefficients 6 and 9). Other high order aberrations, including spherical aberration (coefficient 12), are nearly negligible in every PPL.

Figure 5 shows a 3D representation of the spatially resolved values of the RMS for the three lenses. All aberrations were included except defocus. The behaviour is similar in every PPL, the lower values are in the corridor locations and the higher values in the intermediate peripheral zones. However, spatial differences in the aberration distribution are evident. Lens C shows a more abrupt change between the central and peripheral zones than lenses A and B. Moreover, there are also differences between the nasal and temporal distribution.

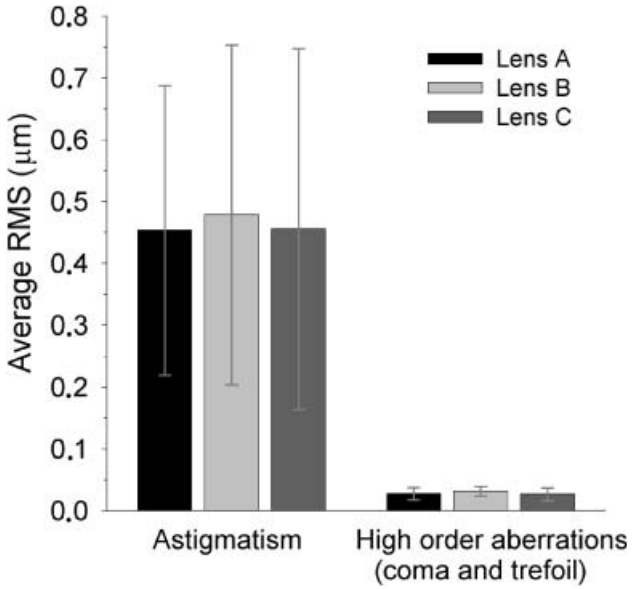

Figure 7. Average RMS of all tested zones of the lenses, for astigmatism and high order aberrations (coma and trefoil) with 4.0-mm pupil diameter. The error bars are the standard deviations. In the case of astigmatism, this parameter denotes how soft or hard the design is.

The amount of aberrations is similar at both sides of lens A, while the temporal side is clearly less aberrated in both lenses B and C.

Figure 6 shows contour plots with iso-RMS lines for two different conditions: (1) only astigmatism and (2) only high order aberrations. The RMS for astigmatism in microns is related to astigmatism in diopters (C) by the following equation:

$$C = \frac{4\sqrt{6}}{r^2}\mathrm{RMS} \quad (1)$$

where r is the radius of pupil in millimetres. Lens B has a lower amount of astigmatism on the temporal side compared with the nasal side, so it is what can be called an asymmetric design. In lens C, this difference is only observed in far and near vision, but not at the intermediate zones. Lens A is the most symmetric design, because there is only a difference between the nasal and temporal sides in the far vision area. In the three tested lenses, larger values of coma and trefoil are found in the corridor where the change of defocus is faster. In far and near areas and in the most peripheral zones, the amounts of these aberrations decrease to half the value in the corridor.

In order to evaluate the amount of total aberration of the lenses, the average RMS values in the 20 zones for astigmatism, coma and trefoil were calculated (*Figure 7*). The average RMS is nearly the same in the three lenses, for both astigmatism and high order aberrations. In addition, standard deviations are also presented. In reference to astigmatism, this parameter reflects how soft or hard a particular design is. Larger standard deviations denote more abrupt changes between central and peripheral zones. Lens A has the lowest value of standard deviation for astigmatism, 0.23 μm, in contrast to 0.27 μm and 0.29 μm for lenses B and C respectively. Following this criterion, lens A is the softest design, while lens C is the hardest.

In any optical analysis of PPLs, it is essential to study the evolution of the addition over the lens. *Figure 8* shows the iso-power lines in the three lenses. The addition distribution is different in the three lenses. For

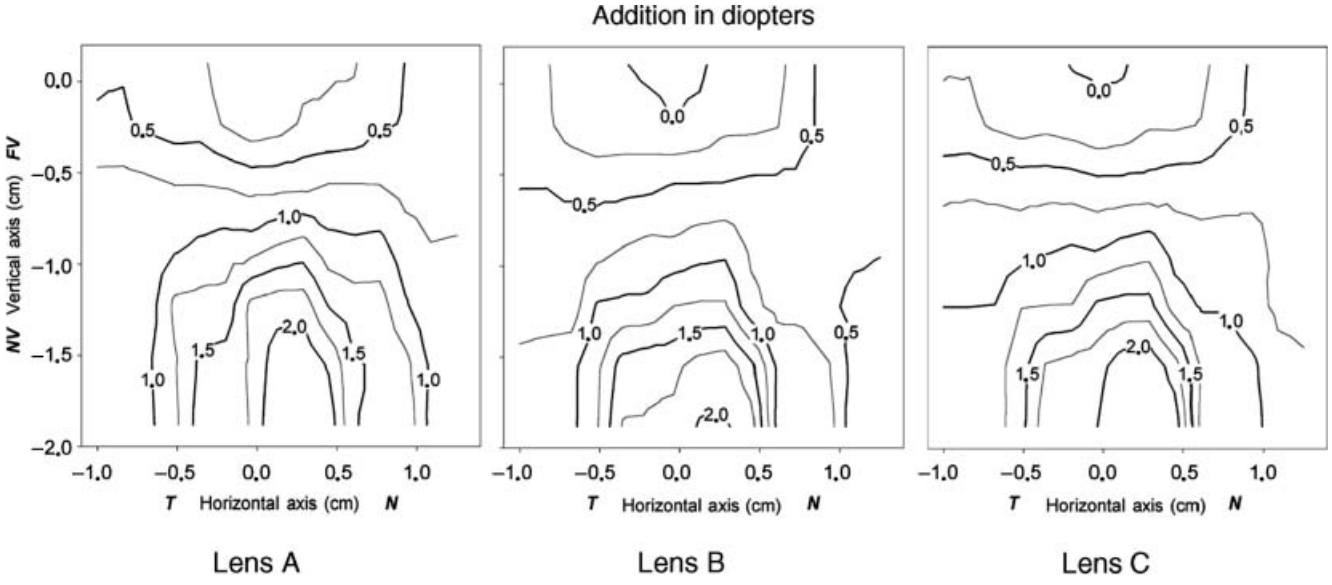

Figure 8. Contour plots of addition for 4.0-mm pupil diameter.

lens A the addition progression begins above the fitting cross, in lens B the complete addition is reached further down, and lens C is an intermediate case. It is interesting to note that although in lens A the spherical power increases faster from far to near zones than in lens B, lens A has a softer design. This is possible because of computer control lathe machines being able to generate any kind of surface design.

Conclusions

In the present paper, the spatially resolved optical performance of three PPLs with different designs has been compared. WAs have been measured in different relevant zones of these lenses. In addition to spatially resolved values of astigmatic and high-order aberrations, the global aberrations of the lenses have also been calculated as the average of the aberration values in all tested locations.

Although, in the last few years, newer designs of PPL have been produced by numerically controlled machines, our results show nearly equal global aberrations for both astigmatism and high order aberrations (coma and trefoil) in three different lenses. The small amounts of coma and trefoil are spatially distributed in a similar way on the three lenses. In the peripheral zones, high order aberrations decrease slightly and coma adopts an oblique orientation because of the distribution of the addition. However, the distribution of astigmatism varies between the tested PPL designs. It depends on lens design philosophy, that is, in which zones the astigmatic aberration is minimized. Peripheral vision has priority in the softer designs, while binocular vision is taken more into account in asymmetrical designs. In this way, the tested PPLs perform like a waterbed, where the astigmatism is the water that can be moved but not eliminated.

References

Alonso, J., GomezPedrero, J. A. and Bernabeu, E. (1997) Local dioptric power matrix in a progressive addition lens. *Ophthalmic. Physiol. Opt*. **17,** 522–529.

Atchison, D. A. and Kris, M. (1993) Off-axis measurements of a plano distance power progressive addition lens. *Ophthalmic. Physiol. Opt*. **13,** 322–326.

Bourdoncle, B., Chauveau, J. P. and Mercier, J. L. (1992) Traps in displaying optical performances of a progressive-addition lens. *Appl. Opt*. **31,** 3586–3593.

Burns, D. (1995) Blur due to pupil area when using progressive addition spectacles. *Ophthalmic. Physiol. Opt*. **15,** 273–279.

Castellini, C., Francini, F. and Tiribilli, B. (1994) Hartmann test modification for measuring ophthalmic progressive lenses. *Appl. Opt*. **33,** 4120–4124.

Cho, M. H., Barnette, C. B., Aiken, B. and Shipp, M. (1991) A clinical study of patient acceptance and satisfaction of Varilux Plus and Varilux Infinity lenses. *J. Am. Optom. Assoc*. **62,** 449–453.

Diepes, H. and Tameling, A. (1988) Comparative investigations of progressive lenses. *Am. J. Optom. Physiol. Opt*. **65,** 571–579.

Fowler, C. W. and Sullivan, C. M. (1989) A comparison of three methods for the measurement of progressive addition lenses. *Ophthalmic. Physiol. Opt*. **9,** 81–85.

Gonzalez, C., Villegas, E. R., Carretero, L. and Fimia, A. (1997) Ronchi test for testing the powers of bifocal intraocular lenses. *Ophthalmic. Physiol. Opt*. **17,** 161–163.

Gresset, J. (1991) Subjective evaluation of a new multi-design progressive lens. *J. Am. Optom. Assoc*. **62,** 691–698.

Han, Y., Ciuffreda, K. J., Selenow, A. and Ali, S. R. (2003) Dynamic interactions of eye and head movements when reading with single-vision and progressive lenses in a simulated computer-based environment. *Invest. Ophthal. Vis. Sci.* **44,** 1534–1545.

Jalie, M. (2001) *Ophthalmic Lenses and Dispensing*. Butterworth-Heinemann, Oxford, pp. 150–163.

Liang, J., Grimm, B., Goelz, S. and Bille, J. F. (1994) Objective measurement of wave aberrations of the human eye with the use of a Hartmann–Shack wave-front sensor. *J. Opt. Soc. Am. A* **11,** 1949–1957.

Liu, L. R. (1994) Contour mapping of spectacle lenses. *Optom. Vis. Sci.* **71,** 265–272.

Loos, J., Greiner, G. and Seidel, H. P. (1998) A variational approach to progressive lens design. *Comput. Aided Design* **30,** 595–602.

Malacara, D. (1992) *Optical Shop Testing*. Wiley, New York.

Minkwitz, G. (1963) Über den Flächenastigmatisms bei gewissen symmetrischen Aspharen. *Optica. Acta.* **10,** 223–227.

Prieto, P. M., Vargas-Martín, F., Goeltz, S. and Artal, P. (2000) Analysis of the performance of the Hartmann–Shack sensor in the human eye. *J. Opt. Soc. Am. A* **17,** 1388–1398.

Quiroga, J. A., Gomez-Pedrero, J. A. and Martinez-Anton, J. C. (2001) Wavefront measurement by solving the irradiance transport equation for multifocal systems. *Opt. Eng*. **40,** 2885–2891.

Rosenblum, W. M., Oleary, D. K. and Blaker, W. J. (1992) Computerized Moire analysis of progressive addition lenses. *Optom. Vis. Sci*. **69,** 936–940.

Rottenkolber, M. and Podbielska, H. (1996) Measuring ophthalmologic surfaces by means of moiré deflectometry. *Opt. Eng*. **35,** 1124–1133.

Sheedy, J. E., Buri, M., Bailey, I. L., Azus, J. and Borish, I. M. (1987) Optics of progressive addition lenses. *Am. J. Optom. Physiol. Opt*. **64,** 90–99.

Spiers, T. and Hull, C. C. (2000) Optical Fourier filtering for whole lens assessment of progressive power lenses. *Ophthalmic. Physiol. Opt*. **20,** 281–289.

Sullivan, C. M. and Fowler, C. W. (1989) Grating visual acuity testing as a means of psychophysical assessment of progressive addition lenses. *Optom. Vis. Sci.* **66,** 565–572.

Tunnacliffe, A. H. (1995) *Essentials of Dispensing*. The Association of British Dispensing Opticians, London, pp. 35–72.

Villegas, E. A. and Artal, P. (2003) Spatially resolved wavefront aberrations of ophthalmic progressive-power lenses in normal viewing conditions. *Optom. Vis. Sci*. **80,** 106–114.